Indian Journal of Engineering & Materials Sciences
Vol. 32, April 2025, pp. 225-238
DOI: 10.56042/ijems.V32i02.14585

Optimization of process parameters in cold metal transfer (CMT) welded dissimilar materials aluminium alloy and coated steel using RSM

Ankush Khansole[a]*, Sushovan Basak[a], Hillol Joardar[a] & Kanwer S Arora[b]

[a]Mechanical Engineering Department, C.V. Raman Global University, Bhubaneswar, Odisha 752 054, India

[b]R&D, Tata Steel Ltd., Jamshedpur, Jharkhand 831 001, India

Received 23 October 2024; accepted: 24 June 2025

Joining of dissimilar materials (AA6061 and zinc-coated steel) has considered the greatest challenge because of poor metallurgical transition at joints. In the present investigation cold metal transfer (CMT) process has been used to improve weld shape and interfacial reaction in-homogeneity of aluminium alloy and galvannealed steel using ER4043 filler wire in lap joint configuration. We have identified three different input process parameters (current, welding speed and weaving length) with three different levels to optimize the process responses (area of bead, leg length and wetting angle). The output or responses have been measured using AutoCAD for all the 20 combinations given by the central composite designs (CCD) model in the response surface methodology technique. The tensile strength of the welded region has been analysed. The mathematical models have been obtained and evaluated for sufficiency using analysis of variance and other steps. The predicted and measured values are relatively identical, suggesting that the established models have been used to accurately predict responses in CMT welding of the Al to HSQ-GA dissimilar metals. The high responses (all) are correlated with the lowest welding speed and the highest degree of current, according to the contour plots of the process parameters. Welding speed has been found to be the most important factor affecting the response variables analysed in the sensitivity analysis.

Keywords: Bead geometry, Pulsed CMT brazing, RSM, Zinc-coated steel

1 Introduction

Dissimilar metals are widely used in automotive industry to reduce the weight of the vehicles which leads to lower fuel consumption and toxic gas emission. Dissimilar aluminium and zinc coated steel joining is very challenging to achieve acceptable weld joint strength due to differences in their melting point, little solubility of Fe in Al and mechanical properties. As a result, brittle intermetallic compounds (IMCs) of Al-Fe generates at interface during welding[1]. Previously many researchers worked on dissimilar metal joining with various fusion welding processes such as metal inert gas brazing (MIGB)[2], gas tungsten arc welding (GTAW)[3-7], laser beam welding (LBW)[8-10] etc. Though, people have tried to join aluminium to steel by solid state welding processes but longer processing time and specific geometries are extremely restricted[11-15].

The cold metal transfer (CMT) process is adopted to overcome the previous issues because it operates on fast responsive control of pulse current, short circuit mode of metal transfer, lower heat input and easy automation[16-19]. It is a modified form of gas metal arc welding (GMAW) process. Because of both the short circuit mode of metal transfer and mechanical retraction filler metal used in CMT which produces less heat than GMA welding. This process is also known as CMT brazing because melting is not occurred at steel side during aluminium to steel dissimilar joining. The deposition rate and bead appearance depends on heat input where current, welding speed, voltage can be varied to get adequate bead geometry and mechanical properties. Due to the lower heat input it can also control the formation of brittle Al-Fe intermetallic compound.

Y. Su *et al.*[20] investigated joint strength of 5052Al alloy and galvanized mild steel using various filler wires such as Al, AlSi5, AlSi12 and Al Mg4.5. It was found that cooling rate has a significant effect on intermetallic layer thickness and higher IMC layer produces weaker joint and better mechanical property was found in Al-Si filler wire compared to Al-Mg filler wire. T Murkami *et al.*[21] joined aluminium to steel dissimilar metals in lap joint configuration using flux cored Al-Si filler wire with MIG arc brazing and stated that the torch position has substantial effect on IMC layer formation and mechanical property. IMC layer thickness of less than 2.5 µm displaced better joint strength with HAZ (aluminium) failure. S. Basak *et al.*[22]

*Corresponding author (E-mail: ankush. Khansole01@gmail.com

studied the diffusivity mechanism, detail microstructure and mechanical properties for pulsed MIG brazed dissimilar joints for automotive grade a6 luminium to galvanealed steel sheets. They achieved 65% (Al base metal) joint strength using AlSi5.

S. Sravanthi *et al*.[23] has done comparative analysis between CMT brazing and MIG brazing of 5052 Al alloy and galvanized mild steel by keeping constant heat input and observed that IMC layer thickness is more in MIGB (7.2 ±0.23µm) compare to CMT braze (6.24 ± 0.23µm). J Singh *et al*.[24] reviewed micro structural and mechanical properties of Al to steel dissimilar joining using MIG-CMT weld brazing. They reported the formation of a brittle intermetallic compound layer at the interface, which mostly consists of $FeAl_3$ and Fe_2Al_5. It can be controlled by optimising the heat input and process parameter, which results in the suppression of the IMC layer. The mechanical properties such as tensile strength, hardness is directly related with bead geometry[19].

Welding parameters interact in complex manner with each other owing to influence on bead geometry.

Optimization was used to achieve the best by performing least. It is important to find optimal process parameter for desired output i.e. weld quality. In optimization, a mathematical model is developed correlating welding process parameters with desired objective function using Design of Experiments, Response surface Methodology and Taguchi method.

S. Shrivastava *et al*.[25] investigated how to minimize bead height and width in IS2062 mild steel joints by optimizing GMAW process parameters (input variables). A RSM model for correlation with input and output responses was built in this study. A four factor three level CCD design matrix was chosen for the optimization purpose. The input welding process parameters namely, wire feed speed, welding speed and gas flow rate were taken into account for the selected output response such as maximum penetration and minimum bead height and width. For increasing penetration depth while keeping. Wire feed speed comes in second, followed by welding speed, with voltage outperforming gas flow rate.

The acceptable joint strength can be obtained with proper welding parameter and filler metal using cold metal transfer technique of dissimilar weld joint. In addition, proposed presetting gap and suitable post weld heat treatment can improve the weld strength. However, increasing the arc torch offset distance reduced the weld strength.

R. Singh *et al*.[26] Investigated the effect of straight polarity and reverse polarity on bead geometry parameters by using the SAW method. RSM makes it easy to build a mathematical model with input variables and responses. CTWD decreases as wire feed speed increases, while bead width increases as welding speed increases. In reverse polarity, bead geometry parameters such as bead width and height, as well as penetration, had higher values than in straight polarity.

M. Islam *et al*.[27] investigated the optimization process parameters using RSM-GA framework to minimize distortion of the weld structure. Four process parameters such as arc voltage, input current, welding speed and welding direction have been optimized for minimum distortion while ensuring sufficient weld penetration. N. Ghosh *et al*.[28] investigated the optimization of GMAW process parameters for butt joining of AISI 316L. The influence of input parameters like welding current, gas flow rate, and CTWD on bead height and width, as well as spread ability. Y. Woolury *et al*.[29] developed a DOE model to predict the weld bead geometry of carbon steel (BMC-16) using P-MIG welding. Pulse current, pulse time, welding speed, background current and background current time period are input variables used, owing to good quality weld bead. They also reported that penetration is affected by the background current and its duration. The optimal parameters are help to achieve good bead weld efficiency.

Appropriate investigations into the analytical approach modelling of various responses (Area, Leg length, and wetting angle) with varying input parameters have not been carried out based on previous work available on the welding of joining of aluminium alloy/steel. Using response surface methodology, the current research attempts to investigate the impact of certain input process parameters on various responses. The influencing parameters were chosen as current, welding speed, and weaving length, and the Face Centred Composite (FCC) design was utilised to collect experimental data and evaluate the effect of these parameters on output responses. RSM was used to construct the second order model between the independent parameters and the responses (output). According to the study, the predicted and experimental values were in excellent agreement.

2 Materials and Methods

2.1 Material

The current study has used a pulsed CMT process with a lap joint to join 2 mm thick aluminium alloy

(Al6061) and 1.2 mm thick gal annealed HSQ steel sheets. The Al6061 and HSQ-GA steel plates were cut from sheet at a size of 100 mm×100 mm, degreased with acetone and clamped properly for CMT welding/brazing. The chemical composition and mechanical properties of the base metal are presented in Table 1. HSQ steel is also known as low carbon steel because it contains 0.098 percent carbon by weight and has a high strength. The filler wire Al-5Si (ER4043) has a diameter of 1.2 mm and is shielded with 99.99% argon at a flow rate of 15 L min^{-1}.

2.2 Process

The Al6061 and HSQ-GA steel plates were cut from sheet at a size of 100mm×100mm, degreased with acetone, and clamped properly for CMT welding/brazing. The CMT process has created a low heat input due to the short circuit technique which has useful to joining of dissimilar metals. Figure 1 shows equipment used in present work i.e. KUKA robot control by CMT2700 of Fronius. Welding parameters given as per DOE and Experiment trial was carried out at different heat input with varying position of torch and welding speed as shown in Table 2.
The heat input for each parameter was calculated by using equation,

$$\text{HI}\ (J\ mm^{-1}) = \eta\frac{60\times IU}{s} \quad \ldots (1)$$

Where, I welding current (A), U Welding Voltage (V), Welding speed s (mm min^{-1}).

Figure1 shows lap joint configuration with 20 mm overlap aluminium is on top side and steel is below side. During experimental work single side lap joint with 20 mm overlap 20º travel angle was maintained. Joint was produced using P-CMT mode set is as shown in Fig.1. After that samples were cut using diamond cutter from the joint and done cold mounting for optimizing bead geometry parameter using AutoCAD.

2.3 Bead geometry

During welding filler wire ER4043 comes in contact with base metal i.e. Al6061 alloy and galvannealed HSQ steel which introduces arc between them. Due to high temperature of arc filler wire get melted then it deposits on joint. This deposition of filler wire called bead or weld shape. The bead appearance and its geometry such as Wetting length, height, width and wetting angle depends on welding parameters like current, welding speed etc. Figure 2 shows bead profile with geometry parameters.

2.4 Tensile strength

To study the load sustaining capacity of welded joint by using shear tensile test. Form the weld joint

Table 2 — Welding parameters with their levels.

Parameters	Unit	Symbol	Level		
			-1	0	+1
Current	Amp	I	40	50	60
Welding speed	mm min^{-1}	WS	50	100	150
Weaving length	mm	WL	1	2	3

Table 1 — Chemical composition and mechanical property of base metals.

Base metal	Chemical composition (%)							Mechanical property		
	C	Cr	Ni	Mn	Fe	Si	Cu	YS (MPa)	UTS (MPa)	El (%)
HSQ	0.098	-	-	1.46	Bal.	0.01	-	346	470	32
Al6061	0.25	0.04	-	0.15	0.7	0.4	0.15	285	334	13.4

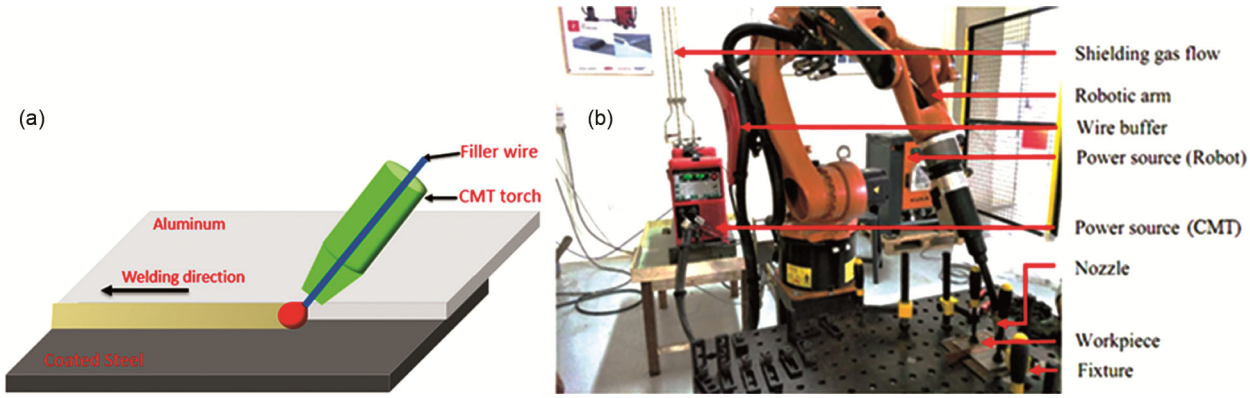

Fig. 1 — (a) Welding join configuration, and (b) CMT machine setup with KUKA robot.

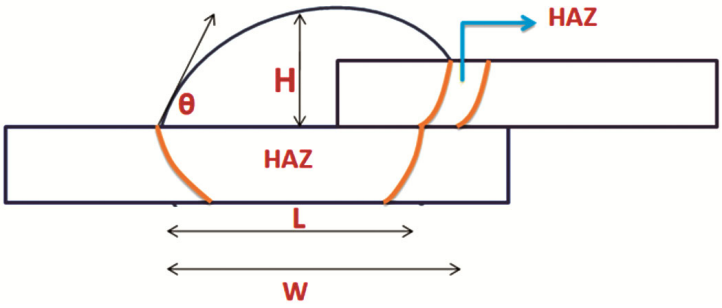

Fig. 2 — Bead profile.

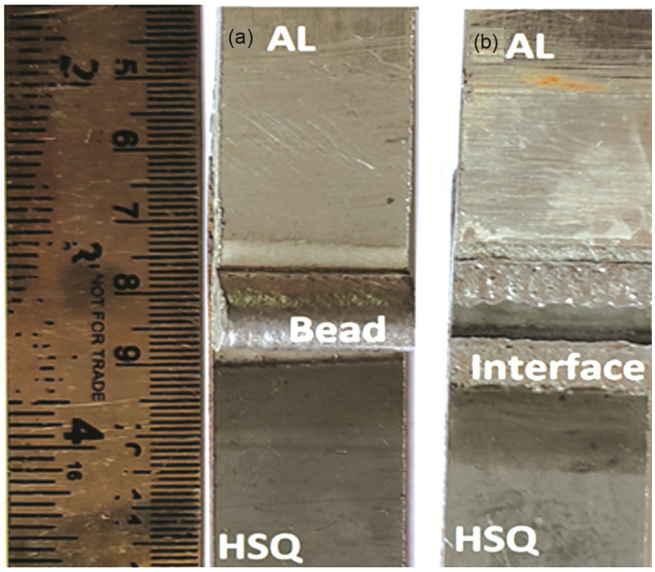

Fig. 3 — (a) Tensile sample before, and (b) after tensile test.

cuts tensile sample by CNC milling having width 15mm shown in Fig. 3. Shear tensile test were carried out at 100KN capacity universal tensile machine (Instron).

2.5 Response surface methodology (RSM)

Central composite designs (CCD) are commonly used in experimentation to investigate the effect of different factors or combinations of factors on a process. In the present study, the face centred composite design matrix consisting of 3 factors (3 levels) design of RSM produced using the 'Mini Tab (V 14)', which has 20 experimental runs displayed in Table 3. The levels of three input welding parameters, as well as their ranges, are shown in Table 2. RSM designs may also be used to calculate the relationships between one or more calculated responses and main input variables. The data obtained must be evaluated in a statistically sound manner using regression in order to decide whether there is a relationship between the factors and the response variables are examined. The independent variables x1, x2, x3……, xk are assumed to be continuous that can be controlled with negligible error. The response 'Y' is considered as a random variable. In most experimental settings, the independent variables that have a functional relationship with response 'Y' can be represented quantitatively. This may be written as[30]:

$$Y = f(x_1, x_2, ...) \pm \varepsilon \quad \ldots (2)$$

where 'ε' measures the experimental error.

In response surface methodology, *'f'* is represented by a second order polynomial in independent variables x_s. This is given by[31]:

$$Y = b_0 + \sum_{i=1}^{k} b_i x_i + \sum_{i=1}^{k} b_{ii} x_i^2 + \sum_{i}^{k} \sum_{j}^{k} b_{ij(i<j)} x_i x_j + \varepsilon \quad \ldots (3)$$

3 Results and Discussion

The front side and back side appearance of joint is achieved by different welding parameters i.e. welding

Table 3 — Design layout and experimental results.

Current (A)	Welding Speed (mm min^{-1})	Weaving length (mm)	Area (mm^2)	Leg Length (mm)	Wetting Angle (θ)	Tensile strength (MPa)
40	50	1	48.47	6.80	130.00	52.98
60	50	1	75.42	11.46	163.28	84
40	150	1	17.09	4.38	109.50	123.74
60	150	1	28.10	6.13	129.50	100.09
40	50	3	39.15	5.75	110.50	58.62
60	50	3	67.35	10.30	144.00	79
40	150	3	19.77	4.95	104.71	107.29
60	150	3	32.05	6.60	124.50	107.66
40	100	2	24.34	5.45	103.06	112.17
60	100	2	42.92	8.53	129.83	117.73
50	50	2	55.96	8.82	131.01	92
50	150	2	23.96	5.85	110.69	105.13
50	100	1	30.96	6.60	126.00	127.66
50	100	3	29.12	6.25	113.22	116.77
50	100	2	31.07	6.90	115.00	129.88
50	100	2	31.77	6.91	114.90	130
50	100	2	31.87	6.80	114.67	132.11
50	100	2	31.97	6.90	115.00	131.9
50	100	2	31.93	6.88	115.00	131.8
50	100	2	31.97	6.90	115.02	132

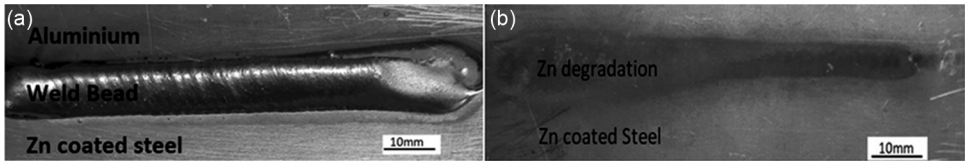

Fig. 4 — (a) Front view of weld sample, and (b) Back view of weld sample.

speed, current and traveling path of welding torch. Figure 4 shows macro image of front side and backside view of CMT Al to HSQ-GA coated steel dissimilar joint in lap position. The front side joint appearance shows a bright, smooth bead profile and without critical defects such as porosity, spatter. On the back side of steel, Zn degradation (evaporation) appeared due to heat concentration exactly below the weld bead. The bead geometry is characterized in terms of bead height (H) from the top of the lower sheet, bead width (W), leg length (L) and cross-section area (A) as shown in Fig. 2. It has been observed that the bead geometry depends on the brazing parameters. Bead geometry also depends on welding process and filler wire composition[32].

Figure 5 represents macro images of bead appearance (front side) of Al to steel brazed joint as per DOE Table 3. It was clearly observed that the welding parameters viz. welding speed, current, and weaving length is significant factor to determine bead shape, appearance and defect free joint. On other hand change in bead width and leg length is also function of weaving length. It helps to increase flowability of molten metal on base metal illustrates increase in leg length and width of bead also shows smoother bead appearance. At lower welding speed 50mm min^{-1}, referring to equation 1 heat input inversely proportional to welding speed results in excessive fluidity of liquid Al on base metal, causing greater rate of deposition, thicker bead shown in Fig. 5 (1,2,5,6,11) unevenness and burn out surfaces. Due to less speed and high heat input arcing energy is more, produces higher amount of molten metal get solidified suddenly and forms a wider and thicker weld bead[33].

At higher speed 150mm min^{-1} bead is thinner and wider and smooth due to lesser time of contact of filler metal and base metal shown in Fig. 5 (3,4,7,8,12) but at moderate speed 100mm min^{-1} bead appears smother, without any notifiable defect shown in Fig. 5 (9,10,13,14,15), acceptable also holds better joint strength upto 132 MPa due to sufficient thickness of reaction layer at Al to steel brazing interface.

Figure 6 shows the bead profile (cross section) of each trial of DOE. The cross section view was drafted using AutoCAD. The rate of deposition or area of

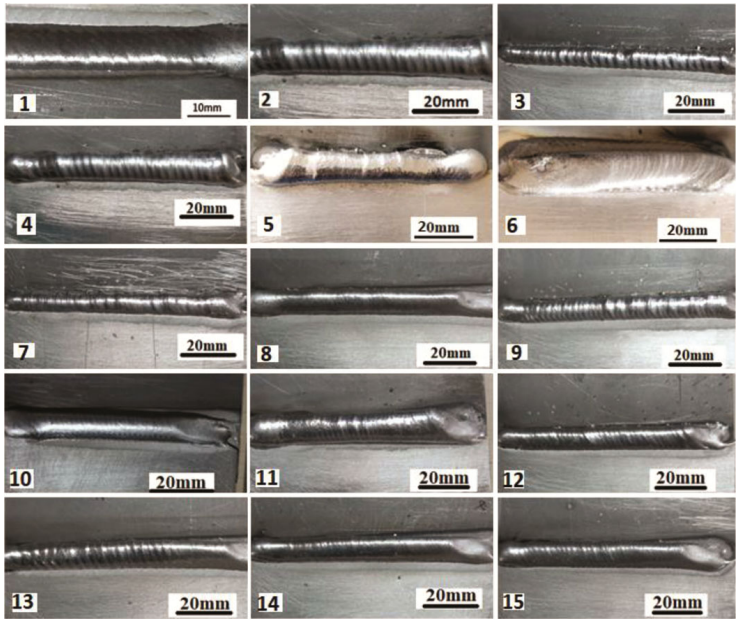

Fig. 5 — Bead appearance (front side) as per DOE experiment.

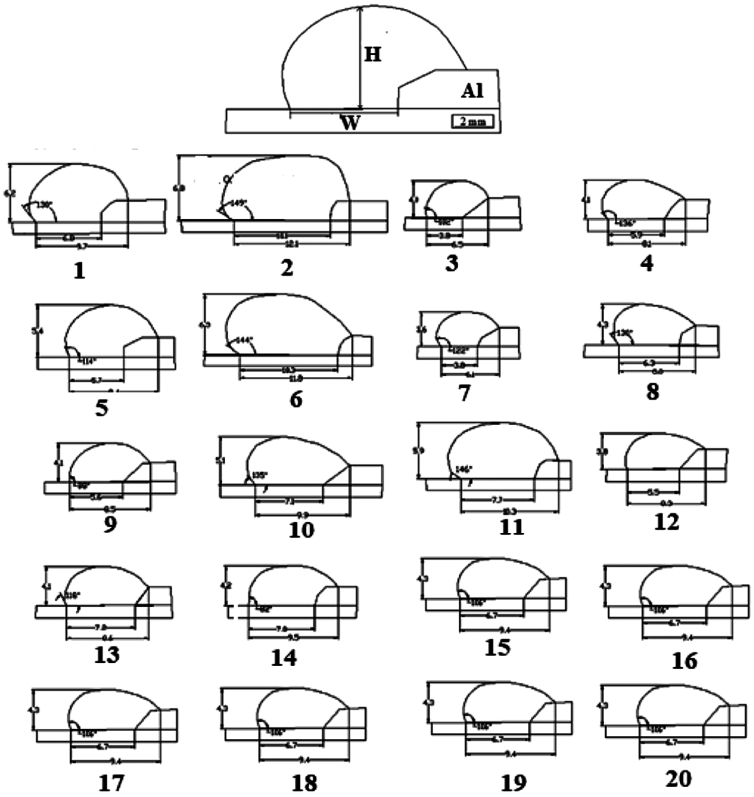

Fig. 6 — Bead geometry (cross section) images as per DOE welding runs.

bead changes with change in CMT weld parameters such as current, welding speed and weaving length. The rate of deposition is the function of the CMT welding parameter. The current increases amount of liquid Al also increases because of high arcing energy.

From Fig. 6, current increases 40 to 60A by keeping constant welding speed 50mm min^{-1} gives an increase in the rate of deposition (increase in area of bead) i.e. 48.4 to 75.4mm^2, same effect in wetting angle 130° to 144° and also same effect found in

welding speed 100mm min^{-1} area of bead increases 24.3, 31, 42.9mm^2 also rise in wetting angle 103°, 115°, 129.8°.

At constant current 40A and different welding speeds 50, 100, 150mm min^{-1} and weaving length 1, 2, 3 respectively results in decreasing area of bead profile 48.4, 24.3, 19.8mm^2 and also decreases wetting length 6.8, 5.4, 4.9 mm. From trial no. 2 and 6, constant current 60A, welding speed 50mm min-1 and change in weaving length 1 to 3 give reduction in wetting angle from 163.2º to 144º and the area of bead 75.4 to 67.3mm^2. The same results were found during trail no. 13, 14 for current 50A and trail no. 1, 5 for current 40A. During trial no. 2, 10, 8 maintain constant current 60A and varying speed 50,100,150mm min^{-1} also change in weaving length 1, 2, 3 shows effect on bead geometry parameters i.e. decrease in area of bead or rate of deposition 48.4, 42.9, 32mm^2 and also decrease wetting angle 130º, 129º, 124.5º respectively. Increase in speed and weaving length results in spreading of bead and reduces wetting angle.

During the joining of dissimilar metals Al to steel produces weld brazed hybrid joint. It means on Al side welding and steel side brazing with Al base filler wire takes place. The intermetallic compound layer was formed at the Al to steel brazed interface which holds joint strength. After observing all the weld joints, current 50A and welding speed 100mm min^{-1} welding parameter gives acceptable results so we go through these parameters. Figure 7 (a-c) shows CMT brazed joint at varying current 40, 50 and 60A keeping constant welding speed 100mm min^{-1} and weaving length 2mm. An increase in welding current heat input also increases, produces an effect on bead geometry parameters and strength of the joint[34].

At low welding current 40A, the heat input is also lower so less amount molten metal produces results in smaller rate of deposition i.e. area of weld bead was less 24.3mm^2 likewise in higher current 50A, 60A heat input is more it means increase in rate of deposition i.e. area of bead is also increasing 31.1mm^2, 42.9mm^2 respectively. The same effect was observed in leg length from Fig. 7, current increases also increase in leg length 5.5, 6.9 and 8.5mm respectively attributed to increase in fluidity of molten metal because of change in heat input with welding current.

Due to small area of bead and leg length the thickness of reaction layer is small so strength is less 112.2MPa because of less thickness of intermetallic layer easily gets crack. At high deposition 42.9mm^2

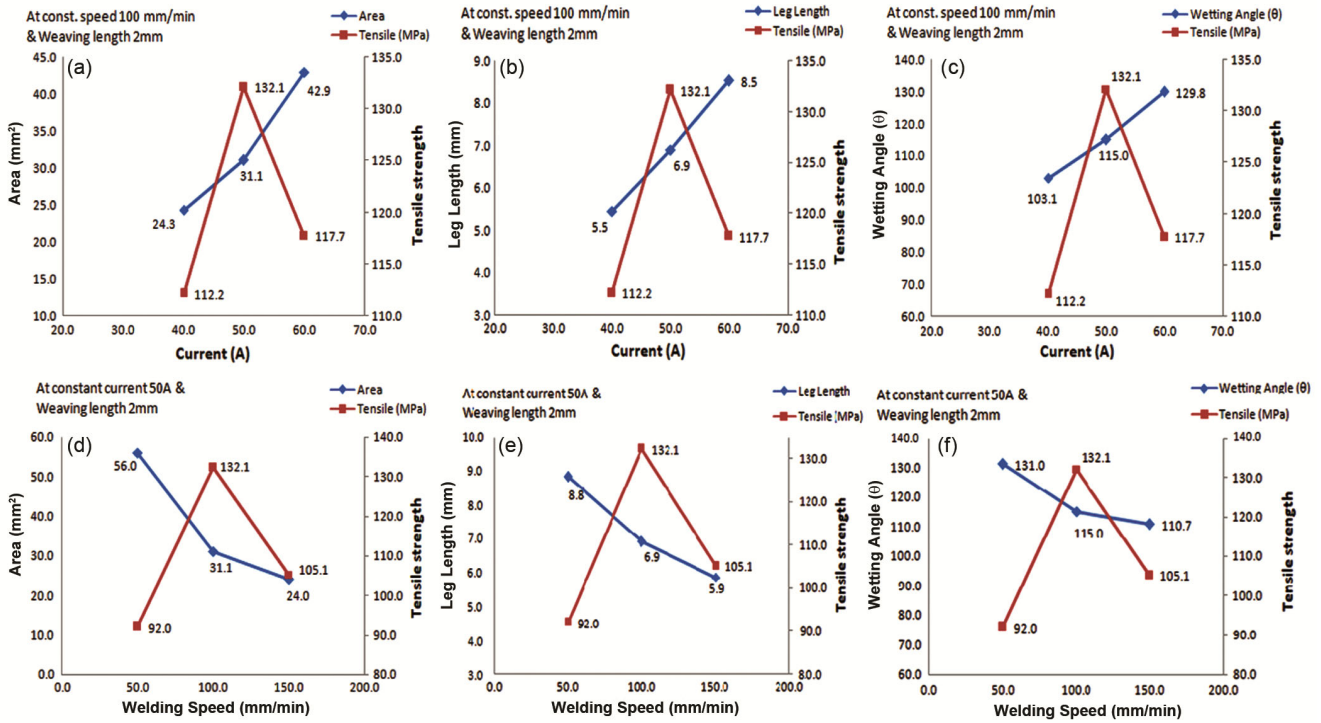

Fig. 7 — Graphical representation of welding process parameter versus bead geometry parameters (a) Current versus Area, (b) Current versus Leg length, (c) Current versus Wetting angle, (d) Welding speed versus Area, (e) Welding speed versus Leg length and (f) Welding speed versus Wetting angle.

increases bead height which is not acceptable. At higher leg length 8.5mm, thicker intermetallic layer was found which is brittle in nature so crack easily propagates and joint gets fail at 117.7MPa. But at moderate area 31.1mm^2 and leg length 6.9mm at 50A current which shows high strength 132.1MPa attributed to medium reaction layer thickness 3µm to 7µm.

Same effect shows in Fig. 7 (c) current increases 40 to 60A also increase in wetting angle from 103° to 129.8°. Wetting is very less then deposition also less so joint strength is less 112.2 MPa due to less deposition. Wetting angle is high 129.8 MPa due to more heat input which enhances flowability of molten metal but joint gets weaker having 117.7MPa. At 50A flowability and spreadabiltiy is good and increase in joint strength 132.1MPa. Figure 7 (d-f) shows relation between welding speed and Area of bead, leg length, wetting angle respectively. Welding speed increases from 50mm min^{-1}, 100mm min^{-1},150 mm min^{-1} rate of deposition i.e. area of bead decreases from 56mm^2, 31.1mm^2, 24mm^2.

The wetting and spreading ability was gradually enhanced with more stable and uniform bead appearance at high heat input. Figure 7 (d-f) illustrates the bead geometry viz. bead area, leg length, wetting angle and tensile strength significantly depends on welding speed. The bead geometry parameters were changes with change in CMT process parameter. As per heat input relation in equation 1, current is directly proportional to heat input. Figure 7(d-f) illustrates strength of CMT brazed joint at varying welding speed 50, 100 and 150mm min^{-1} keeping constant welding current 50A and weaving length 2mm. At low welding speed, area of bead is higher due to high heat input and higher rate of deposition. The height bead high so it gives less strength is also less 92MPa. An enhancement in welding speed 150mm min^{-1} decrease in rate of deposition because no longer arcing time so area of bead also reduces 24mm^2 which effect in less strength 105.1MPa. But at moderate speed 100mm min^{-1} rate of deposition and strength is good i.e. 132.1MPa. Welding speed also shows relative effect on leg length. Welding increases leg length decreases due to less solidification time. Leg length is high 8.88mm at low speed 50mm min^{-1} then thick IMC layer was produced which is brittle in nature so joint gets cracked. It also gives less strength 92MPa. At high speed 150mm min^{-1}, leg length is small then thinner IMC layer produced at interface crack propagates easily results in joint get fail at less strength 105MPa. At 100mm min^{-1} leg length is 6.9mm which produces proper IMC layer having 3.9-6µm and hold good joint strength 132.1MPa. Same effect shows in Fig. 7f welding speed increases 50, 100, 150mm min^{-1} wetting angle decreases 131°, 115°, 110°due to increases in heat intensity spreading of molten metal. At high angle width is less and height is more so thin IMC layer get cracked and at very low wetting angle due to high heat input brittle IMC layer crack easily propagated and also shows less strength 105MPa.

The statistical variables were analysed and record the result. Summary of developed model as shown in above Table 3. Each response models have been mathematically modelled using regression coefficients and statistical analysis using the predicted value of each response. Table 4 displays the regression coefficients for various response models. From the Table 4, the models are shown as:

$$\text{Area} = 73.4028 - 0.40121 - 0.7325WS - 1.5633WL + 0.0217I^2 + 0.0034WS^2 - 1.4256WL^2 - 0.008I.WS + 0.0601WS.WL \quad \ldots (4)$$

$$\text{Length} = 0.1604 + 0.1718I - 0.012WS + 0.7708WL + 0.0013I2 + 0.0002WS^2 - 0.4338WL2 - 0.0015I.WS + 0.0081WS.WL \quad \ldots (5)$$

$$\theta = 141.0667 + 0.5068I - 0.4794WS - 32.0389WL + 0.015I2 + 0.0024WS^2 + 4.6617WL2 - 0.0067I.WS + 0.0725WS.WL \quad \ldots (6)$$

The analysis of variance (ANOVA) was used to determine the statistical significance of the complete quadratic models that were anticipated. The significance and extent of each variable's effects, as well as all of their linear, quadratic, and interaction effects, were also calculated. The lack-of-fit test was used to ensure that the completed quadratic model was fit correctly. The result of the quadratic models for area, leg length and wetting angle are shown in Table 2. Table 2 also shows that all of the response

Table 4 — Regression coefficient of various responses.

Term	Area (mm^2)	Length (mm)	Theta (°)
Constant	73.4028	0.1604	141.0667
I	-0.4012	0.1718	0.5068
WS	-0.7325	-0.0120	-0.4794
WL	-1.5633	0.7708	-32.0389
I*I	0.0217	0.0013	0.0150
WS*WS	0.0034	0.0002	0.0024
WL*WL	-1.4256	-0.4338	4.6617
I*WS	-0.0080	-0.0015	-0.0067
WS*WL	0.0601	0.0081	0.0725

terms in equations 4, 5, and 6 are meaningful since the p-values associated with these terms are less than 0.05. From the ANOVA table for quadratic model, when the estimations of "p" ("Prob. > F") for the term of models are under 0.05 (i.e. $\alpha = 0.05$, or 95% confidence level), this shows the procured models are taken as statistically imperative, which is desirable. I.WL two-way interaction model terms is not significant for all the response. These non-essential model terms may be removed for potentially improving the model. Tables (5-7) show the ANOVA table for the diminished quadratic model for three responses, using the backward elimination technique to naturally minimize the terms that are not important. Tables (5-7) demonstrate that the models are still significant and it likewise shows that the trial of lack-of-fit is not decisive. R2, which is referred to as determination coefficients in the following ANOVA table, is defined as the proportion of explained variation to total variation and is used to determine the degree of fit. The closer R2 gets to unity, the better the reaction display matches the real data. It means that the less difference between expected and actual values is better. It is also found that there is a strong correlation between the experimental and expected values, as demonstrated by high R2 values. This shows that all of the models are significant.

The residuals in the plots in Fig. 8a, 9a, and 10a typically fall on a straight line, indicating that the errors are distributed normally. Also, Fig. 8b, 9b and 10b revealed that they have no obvious pattern and unusual structure. This means that the models presented are sufficient, and there is no reason to assume that the independence or constant variance assumptions have been violated.

Figures 11a, 12a, 13a show contour plot of bead geometry and input parameters. Figures 11b, 12b, 13b show graphical representation of input & output variables in which x axis and y axis are represents input variables i.e. current and welding speed and z axis gives response or result variables i.e. bead geometry parameters. The area of counter plot gives value response variable; z axis shows response of x axis and y axis. In Fig. 11 (a &b) current increases with increase in area of bead. Figure 12 & Fig. 13 shows current increases slightly increase spreadability of joint i.e. leg length, wetting angle.

Table 5 — Analysis of variance for area.

Terms	DF	Seq SS	Adj SS	Adj MS	F	P
Regression	8	4305.49	4305.49	538.19	1895.42	0.000
Linear	3	3692.47	3692.47	1230.82	4334.79	0.000
Square	3	414.03	414.03	138.01	486.0	0.000
Interaction	2	198.99	198.99	99.50	350.41	0.000
Residual Error	11	3.12	3.12	0.28		
Lack-of-Fit	6	2.52	2.52	0.42	3.47	0.097
Pure Error	5	0.61	0.61	0.12		
Total	19	4308.62				

Table 6 — Analysis of variance for length.

Terms	DF	Seq SS	Adj SS	Adj MS	F	P
Regression	8	54.4943	54.4943	6.8118	3148.63	0.000
Linear	3	48.0149	48.0149	16.005	7398.04	0.000
Square	3	0.9460	0.9460	0.3153	145.75	0.000
Interaction	2	5.5334	5.5334	2.7667	1278.86	0.000
Residual Error	11	0.0238	0.0238	0.0022		
Lack-of-Fit	6	0.0152	0.0152	0.0025	1.48	0.341
Pure Error	5	0.0086	0.0086	0.0017		
Total	19	54.5181				

3.1 Equations of sensitivity analysis

Area - Area of weld bead
WS - Welding speed
WL -Weaving length
θ – Wetting angle
Length- Wetting length (Leg length)

$$\frac{\partial\,(\text{Area})}{\partial\,(\text{WS})} = -0.7325 + 0.0068\,\text{WS} - 0.008\,\text{I} + 0.0601\,\text{WL} \quad \ldots (7)$$

$$\frac{\partial\,(\text{Area})}{\partial\,(\text{I})} = -0.4012 + 0.0434\,\text{I} - 0.008\,\text{WS} \quad \ldots (8)$$

Table 7 — Analysis of variance for theta.

Terms	DF	Seq SS	Adj SS	Adj MS	F	P
Regression	9	3902.32	3902.32	433.59	12099.56	0.000
Linear	3	3152.20	3152.20	1050.73	29321.23	0.000
Square	3	554.11	554.11	184.70	5154.19	0.000
Interaction	3	196.01	196.01	65.34	1823.27	0.000
Residual Error	0.10	0.36	0.36	0.04		
Lack-of-Fit	5	0.27	0.27	0.05	2.89	0.134
Pure Error	5	0.09	0.09	0.02		
Total	19	3902.68				

$$\frac{\partial\,(\text{Area})}{\partial\,(\text{WL})} = -1.563 - 2.8512\ \text{WL} + 0.0601\ \text{WS} \quad \ldots (9)$$

$$\frac{\partial\,(\text{Length})}{\partial\,(\text{WS})} = -0.012 + 0.0004\ \text{WS} - 0.0015\ \text{I} + 0.0081\text{WL} \quad \ldots (10)$$

$$\frac{\partial\,(\text{Length})}{\partial\,(\text{I})} = 0.1718 + 0.0026\text{I} - 0.0015\text{WS} \quad \ldots (11)$$

$$\frac{\partial\,(\text{Length})}{\partial\,(\text{WL})} = 0.7708 - 0.8676\text{WL} + 0.0081\text{WS} \ldots . (12)$$

$$\frac{\partial\,(\theta)}{\partial\,(\text{WS})} = -0.4794 + 0.0048\text{WS} - 0.0067\text{I} + 0.0725\text{WL} \quad \ldots (13)$$

$$\frac{\partial\,(\theta)}{\partial\,(\text{I})} = 0.5068 + 0.030\text{I} - 0.0067\text{WS} \quad \ldots (14)$$

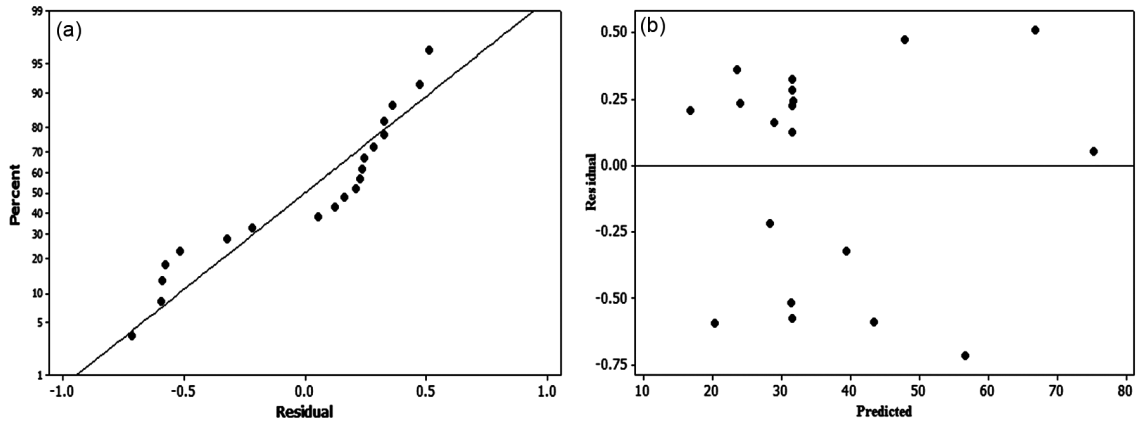

Fig. 8 — (a) Normal probability plot of residuals for area, and (b) Plot of residuals versus predicted response for area.

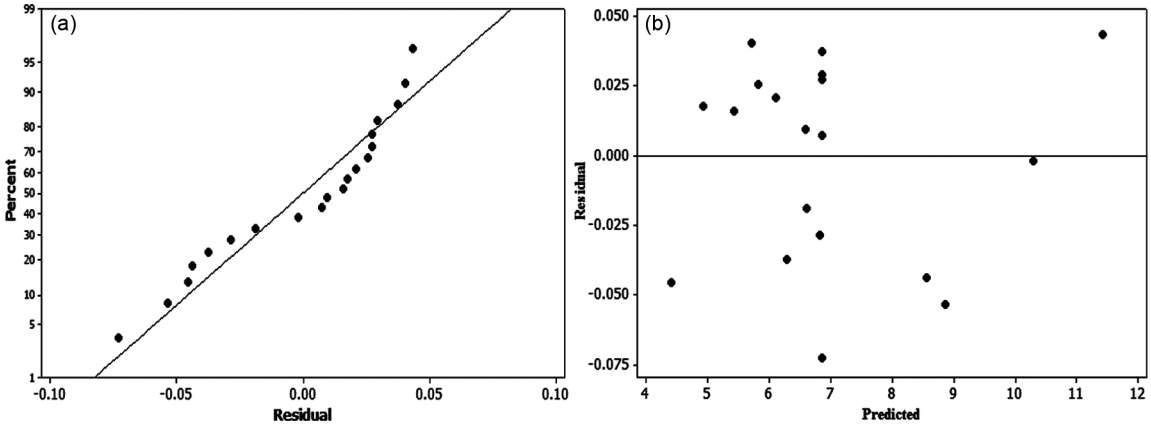

Fig. 9 — (a) Normal probability plot of residuals for leg length, and (b) Plot of residuals versus predicted response for leg length.

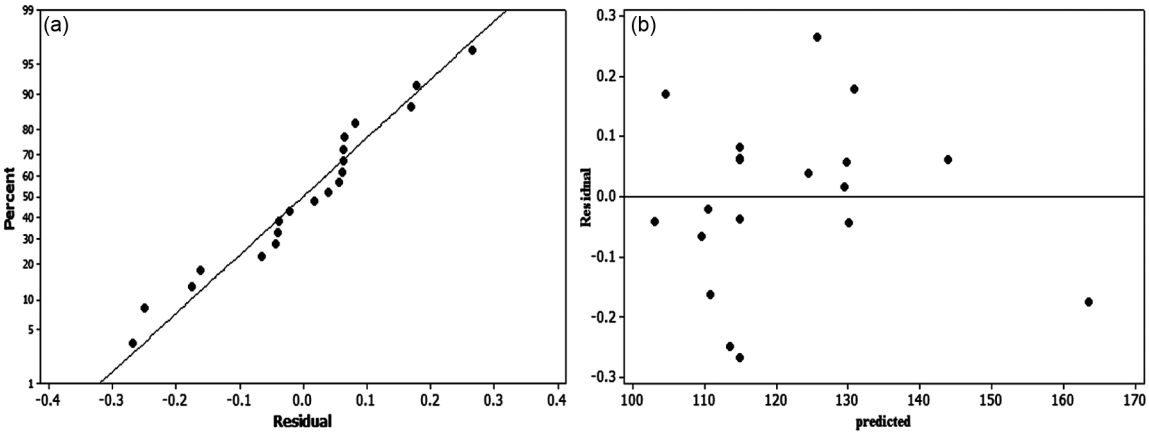

Fig. 10 — (a) Normal probability plot of residuals for wetting angle, and (b) Plot of residuals versus predicted response for wetting angle.

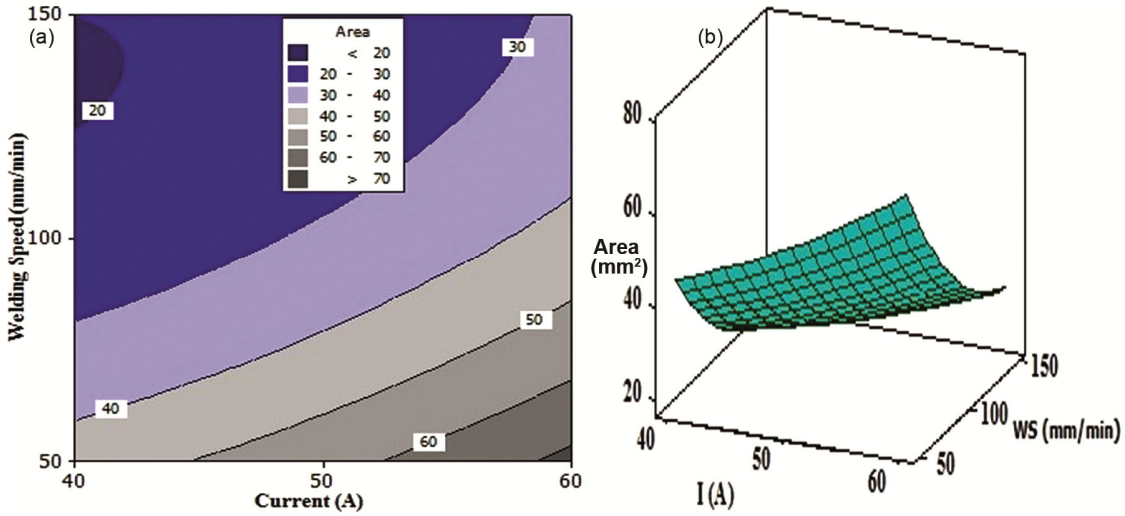

Fig. 11 — Area (a) Contours, and (b) Surface plot in welding speed–current at weaving length of 2.

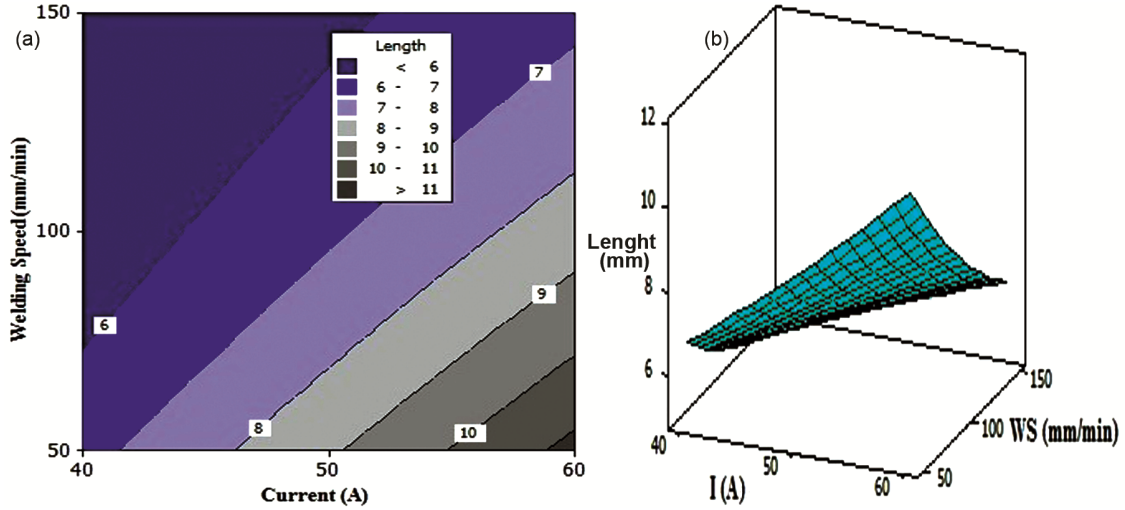

Fig. 12 — Leg Length (a) Contours, and (b) Surface plot in welding speed–current at weaving length of 2.

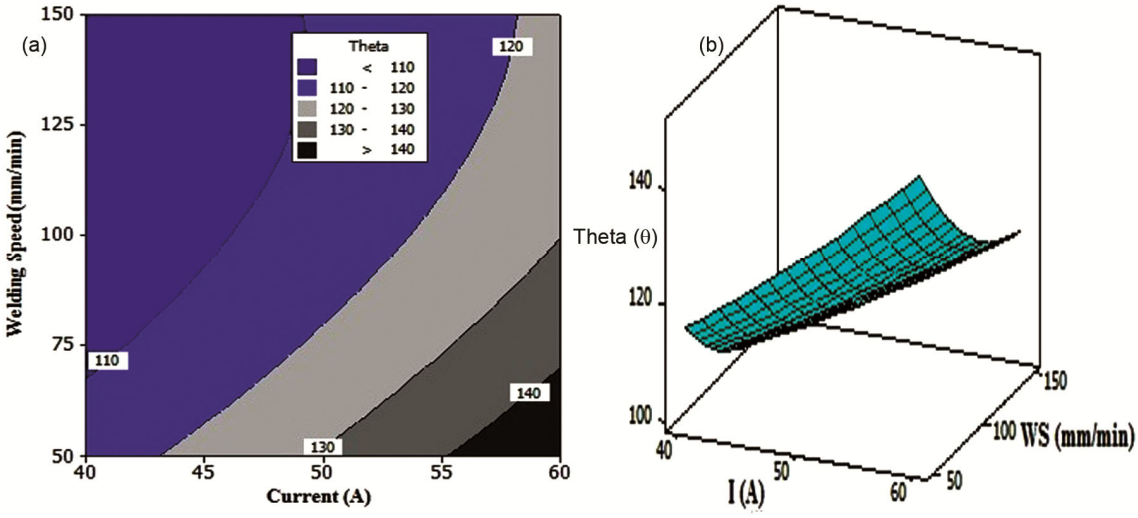

Fig. 13 — Wetting angle (a) Contours, and (b) Surface plot in welding speed–current at weaving length of 2.

$$\frac{\partial(\theta)}{\partial(\mathrm{WL})} = -32.0389 + 9.332\mathrm{WL} + 0.0725\mathrm{WS} \quad \ldots (15)$$

3.2 Sensitivity analysis

Sensitivity analysis, a method for defining important parameters and rating them by their importance, is critical in model validation, where attempts are made to equate calculated output to measured results. Sensitivity analysis is conducted to investigate the sensitivity of the chosen output (area of weld bead, wetting length, wetting angle) to the selected design variables (welding speed, current and weaving length).

This method of analysis will look at the parameters need to be calculated the most precisely, resulting in a list of the input parameters that have the most impact on model outputs[36,36]. The partial derivative of a design objective function with respect to its variables is the sensitivity of that function with respect to a design variable in mathematics. Equations. (4), (5), and (6) are separated with respect to current to obtain the sensitivity equations. The sensitivity Equations (7) – (15) represent the sensitivity of area of weld bead, wetting length and wetting angle for welding speed, current and weaving length respectively.

The purpose of this research work is to forecast the tendency of output responses due to changes in CMT process parameters. Table 8 and Figs (14-16) show the sensitivity of cross section area of bead, wetting length, and wetting angle to welding speed, current, and weaving length as estimated from Eqs (7-15) respectively.

From the Fig. 14 (a &b), it has been seen that the area of weld bead is found sensitive with respect of welding speed and current with the variation of current. Similar results are found wetting length with respect of welding speed and wetting angle with respect of welding speed and current with the small variation of current (Fig. 15a, 16a and 16b respectively). But area of the weld bead, wetting length and wetting angle with respect of weaving length is not sensitive with the variation of current (Fig. 14c, 15c and 16c). The results reveal that the all the responses (output) are more sensitive to welding speed than current and weaving length.

Table 8 — Sensitivity analysis as per equations (7 – 15).

Sensitivity

Speed (mm min^{-1})	Current (A)	Area of weld bead			Wetting length			Wetting angle		
		$\frac{\partial(\text{Area})}{\partial(\text{WS})}$	$\frac{\partial(\text{Area})}{\partial(\text{I})}$	$\frac{\partial(\text{Area})}{\partial(\text{WL})}$	$\frac{\partial(\text{Length})}{\partial(\text{WS})}$	$\frac{\partial(\text{Length})}{\partial(\text{I})}$	$\frac{\partial(\text{Length})}{\partial(\text{WL})}$	$\frac{\partial(\theta)}{\partial(\text{WS})}$	$\frac{\partial(\theta)}{\partial(\text{I})}$	$\frac{\partial(\theta)}{\partial(\text{WL})}$
50	40	-0.7313	-0.4366	-1.6231	-0.0109	0.1707	0.7627	-0.4175	0.4835	-32.1114
	50	-0.7393	-0.3932	-1.6231	-0.0124	0.1733	0.7627	-0.4842	0.5135	-32.1114
	60	-0.7473	-0.3498	-1.6231	-0.0139	0.1759	0.7627	-0.5509	0.5435	-32.1114
100	40	-0.7245	-0.4446	-1.563	-0.0105	0.1692	0.7708	-0.4127	0.4768	-32.0389
	50	-0.7325	-0.4012	-1.563	-0.012	0.1718	0.7708	-0.4794	0.5068	-32.0389
	60	-0.7405	-0.3578	-1.563	-0.0135	0.1744	ss0.7708	-0.5461	0.5368	-32.0389
150	40	-0.7177	-0.4526	-1.5029	-0.0101	0.1677	0.7789	-0.4079	0.4701	-31.9664
	50	-0.7257	-0.4092	-1.5029	-0.0116	0.1703	0.7789	-0.4746	0.5001	-31.9664
	60	-0.0012	-0.3658	-1.5029	-0.0131	0.1729	0.7789	-0.5413	0.5301	-31.9664

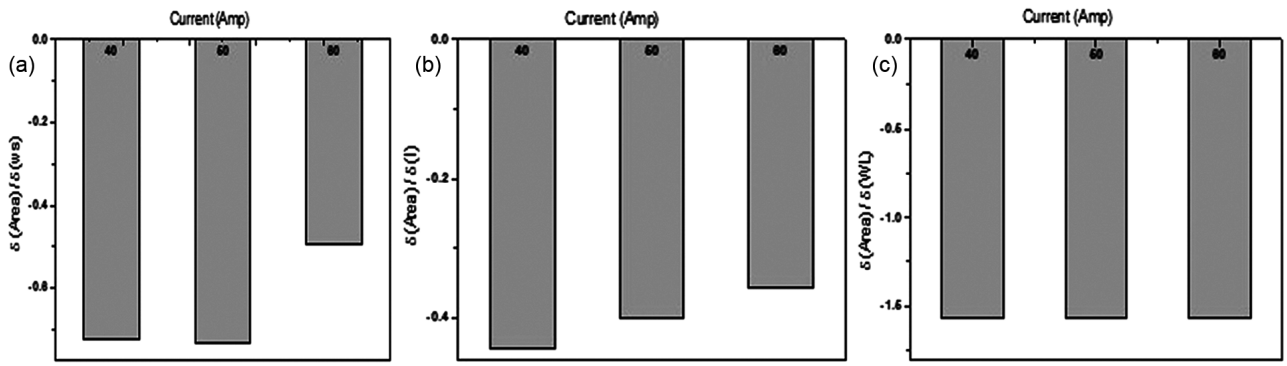

Fig. 14 — Sensitivity analysis result on area of weld bead (a) Welding speed, (b) Current and (c) Weaving length.

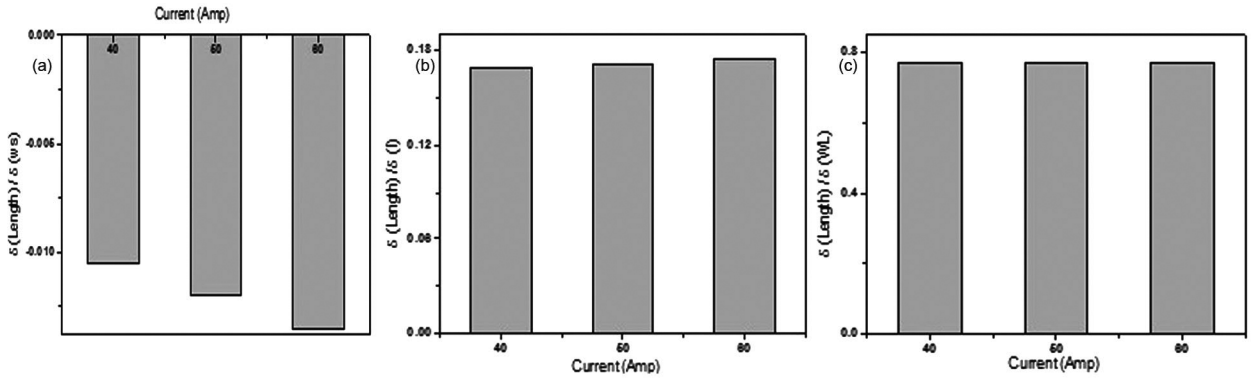

Fig. 15 — Sensitivity analysis result on wetting length (a) Welding speed, (b) Current and (c) Weaving length.

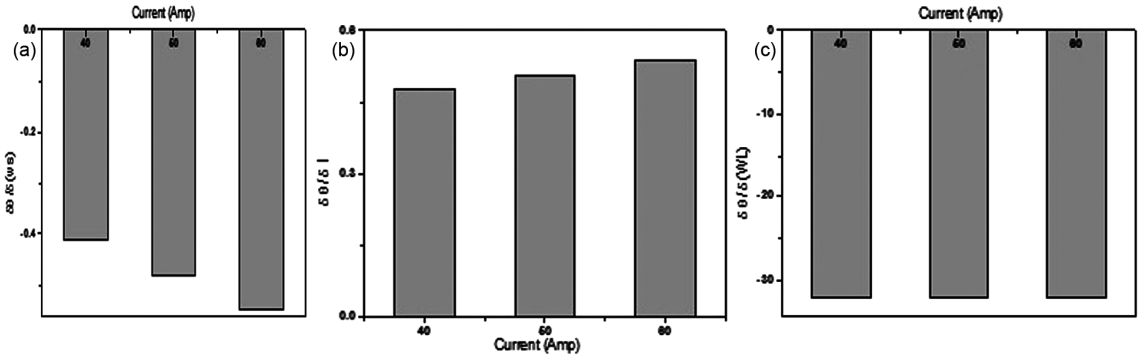

Fig. 16 — Sensitivity analysis result on wetting angle (a) Welding speed, (b) Current, and (c) Weaving length.

4 Conclusion

In present work, aluminium to steel dissimilar joining has been performed using AlSi5 filler wire by CMT process for optimization and analysis of bead geometry process parameter. Significantly, CMT process parameter such as current, welding speed, wire feed speed and CTWD has puts vital importance in bead appearance and spreading behaviour of weld pool.

In this paper, Al to steel dissimilar joining in lap joint weld runs has been performed using AlSi5 filler wire by CMT process. The plan of optimization and analysis of bead geometry is elaborated. Significant process parameter affecting the bead appearance and spreading of weld metal arc (molten metal or liquid Al) identified as current, welding speed and weaving length.

Bead geometry parameters i.e. response variables to predict weld quality has been found out on the basis of bead appearance, bead geometry and tensile strength. Experiments were done as per DOE matrix three by three level and record the data. The response variables are optimized on the basis of RSM, mathematical model developed and validated. The response variables based on the criteria maximum tensile strength and minimum width and height. The recorded result to found optimal bead geometry parameters.

It is concluded that RSM is powerful tool for optimization of CMT process parameter.

RSM has proved to be an effective tool to predict responses as well as to optimize process parameters for CMT weld brazing. Experimental result of bead geometry that is leg length, width, height and wetting angle from aluminium to steel joint were used to develop responses. Optimized responses 95% of their experimental values. The optimized CMT process parameters give maximum tensile strength 132MPa.

References

1 Yang J, Li YL, Zhang H, Guo W, David W & Zhou N, *Metall Mater Trans A,* 46 (2015) 5149.

2 Mathieu A, Shabadi R, Deschamps A, Suery M, Mattei S, Grevey D & Cicala E, *Opt Laser Technol*, 39 (2005) 652.

3 Lin S B, Song J, Chao G & Yang C,*Front Mater Sci China*, 3 (2009) 78.

4 Song J L, L in S B, Yang C L & Fan C L, *J Alloys Compd*, 488 (2009) 217.

5 Song J L, Lin S B, Yang C L, Fan C L & Ma GC, *Adv Weld Produc Technol*, 15 (2010) 213.

6 Pouranvari M & Abbasi M, *J Alloys Compd*, 749 (2018) 121.

7 Das A, Shome M, Das C R, Goecke Sven- F&De A, *Sci Technol Weld Join,* 20 (2015) 402.

8 Dharmendra C, Rao K P, Wilden J & Eich S, *Mater Sci Eng A*, 528 (2011) 1497.

9 Song N, Chen Su, Honggang D, Dongsheng Z, Xiaosheng Z & Xin Wang G, *J Mater Eng Perform*, 25 (2016)1839.
10 Das A, Shome M, Goecke S F & De A, *Sci Technol Weld Join*, 21 (2016) 303.
11 Das H, Basak S, Das G & Pal T K, *Int J Adv Manufac Technol*, 64 (2013) 1653.
12 Ogura T, Saito Y, Nishida T, Yoshida T, Omichi N, Fujimoto M & Hirose A, *Scr Mater*, 68 (2012) 531.
13 Lee W, Schmuecker M, Mercardo U A, Biallas G & Jung S, *Scr Mater*, 55 (2006) 355.
14 Miller W S, Zhuang L, Bottema J& Wittebrood AJ, *Mater Sci Eng*, 280 (2000) 37.
15 Hovorun TP, Berladir K V, Pererva V I,Rudenko S G & *Martynov A I, J Eng Sci*, 4 (2017) 8.
16 Zhang H T, Feng J C & He P*, Mater Sci Technol*, 24 (2008) 1346.
17 Yagati K, Bathe R, Joardar H, Phaniprabhakar K & Padmanabham G, *Trans Indian Inst Met*, 72 (2019) 2763.
18 Feng J, Zhang H & He P, *Mater Des*, 30 (2009) 1850.
19 Sharma A, Soon-Jae L, Du-Y C & Jae P J, *J Mater Process Technol,* 249 (2017) 212.
20 Sua Y, Huaa X & Wu Y, *JMater Process Technol*, (2014) 750.
21 Murakami T, Nakata K, Tong H & Ushio Masao, *ISIJ International*, 43 (2003) 1596.
22 Basak S, Das H, Pal T K & Shome M, *Mater Character*, 112 (2016) 229.
23 Sravanthi S S,Acharyya S, Phani Prabhakar K V & Padmanabham G, *J Mater Process Technol*, (2019) 1.
24 Singh J, Arora K S&Shukla D K, *J Alloys Compd*, 784 (2019) 753.
25 Srivastava S & Garg K, *J Manufac Process,* 25 (2017) 296.
26 Singh R P, Gar R K & Shukla D K*, J Manufac Process*, 21 (2016)14.
27 Islam M, Buijk A, Rohani M R& Motoyama K, *Adv Eng Software*, 79 (2015) 127.
28 Ghosh N, Pal RK & Nandi G, *Sci Technol*, 25 (2016) 238.
29 Wooluru Y, SD R & Rangaswamy J, *Int J Appl Eng Res*, (2018) 13.
30 Lendvai A, *J Mater Sci,* 5 (1986) 1219.
31 Donga H, Hua W, Duana Y, Wanga X & Dong C, *J Mater Process Technol*, 212 (2012) 458.
32 Choudhary DK, Jindal S &Mehta N P, *Elixir Mech Eng*, 40 (2011) 5519.
33 Chen Z, Chang Li, Han X& Cao X, *J Adhesion Sci Technol*, (2020) 1.
34 Kim I S, Son K J, Yang Y S &Yaragada P, *Int Machine Tools Manuf*, 43 (2003) 763.
35 Li J, Li H, Wei H.&Ni Y, *Int J Adv Manuf Technol*, 84 (2016) 705.
36 Bouche K, Barbier F & Coulet A, *Mater Sci Eng*: *A*, 249 (1998)167.